

Studies on spectral, dielectric and nonlinear optical properties of L-alanine alaninium picrate (LAAP) crystals

P. SELVARAJAN*, R. JOTHI MANI, D. SHANTHI

Department of Physics, Aditanar College of Arts and Science, Tiruchendur-628216, Tamilnadu, India

L-alanine is one of the simplest amino acids like glycine and it is a non-centrosymmetric crystal. Its nonlinear optical (NLO) property is highly pronounced when L-alanine is mixed with a non-centrosymmetric organic acid such as picric acid. In this work, L-alanine alaninium picrate (LAAP) salt was synthesized by making reaction between L-alanine and picric acid. Single crystals of LAAP salt were grown by slow evaporation technique. XRD studies reveal the monoclinic structure of the sample. EDAX study was used to identify the elemental composition of the grown crystal. Etching studies were carried out to see the etch pit patterns of LAAP crystal. Second-order and third-order studies were carried out for LAAP sample to analyze the nonlinear optical activity. UV-visible transmittance spectrum of LAAP crystal was recorded to find transparency and optical cut-off wavelength. Also dielectric studies were carried out to observe the electrical processes that are taking place in the LAAP crystal.

(Received February 12, 2014; accepted June 24, 2015)

Keywords: Organic compounds, Optical materials, Crystal growth, X-ray diffraction, Second-order NLO, Third-order NLO, Dielectric properties

1. Introduction

Amino acids and their complexes are second-order or third-order nonlinear optical (NLO) materials that are useful in laser technology, optical communication, optical computing and opto-electronic technologies. These compounds containing amino groups and carboxylic acid groups and they are generally soluble in water and insoluble in non-polar organic solvents such as hydrocarbons. In a zwitterionic form, an amino acid contains positively charged ammonium ion (NH_3^+) and negatively charged carboxylate ion (COO^-) and it has no net charge [1,2]. If the amino group is attached to the position of alpha carbon, it is called an alpha amino acid and L-alanine is an alpha amino acid with the chemical formula $\text{CH}_3\text{CHNH}_2\text{COOH}$. It is a white odorless crystal powder and easily dissolves in water, slightly dissolves in alcohol and undissolves in ether. L-alanine is a conditionally essential amino acid and it is an important source of energy for muscle tissue, the brain and central nervous system. L-alanine strengthens the immune system by producing antibodies, helps in the metabolism of organic acids and sugars and is used by protein synthesis and immune system regulation. It is the simplest acentric crystal with second harmonic generation efficiency of about 0.3 times that of the well known KDP [3-5]. Crystals of L-alanine complexes have been studied by many researchers and reported in the literature [6-12]. Picric acid, also called as 2,4,6-trinitrophenol, is a pale yellow, odourless crystalline solid that crystallizes in a non-centrosymmetric system. Considering the importance of L-

alanine, a research programme is being carried out in our laboratory to study various L-alanine complexes. In this work, L-alanine is mixed with picric acid to form L-alanine alaninium picrate (LAAP) crystal. The aim of this work is to report the nonlinear optical (NLO) and other properties of the grown crystals of LAAP and the results are discussed.

2. Synthesis and growth

In the present study, the commercially available Analar Reagent (AR) grade salts of L-alanine and picric acid were purchased (Merck India) and dissolved in double distilled water in 1.5:1 molar ratio to obtain the synthesized LAAP salt by conventional chemical reaction method. Here the reactants of solution was heated at 60 °C for two or three days till the synthesized salt of LAAP was obtained and it was purified by re-crystallization process twice. The saturated solution of re-crystallized salt of LAAP has been prepared and the solution was stirred well using a hot plate magnetic stirrer for 2 hours and then it was filtered using a Whatmann filter paper. The filtered solution was allowed to evaporate and numerous tiny crystals were formed at the bottom of the container due to spontaneous nucleation. A good quality seed crystal was kept in the supersaturated solution in a beaker and this arrangement was placed in a constant temperature bath (accuracy: 0.01 °C) maintained at 32 °C. Due slow evaporation, the seed crystal was turned into a big-sized crystal. It took about 20 days to grow LAAP crystal of

size $21 \times 15 \times 7 \text{ mm}^3$. Similar procedure was followed to obtain many LAAP crystals for the characterization studies. The photograph of a harvested crystal is shown in the Fig. 1.

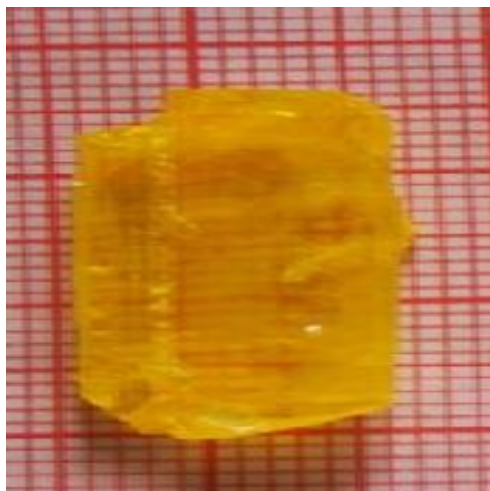


Fig. 1. The grown crystal of LAAP.

3. Techniques for characterization

An ENRAF NONIUS CAD-4 X-ray diffractometer with MoK_α ($\lambda = 0.71069 \text{ \AA}$) radiation was used to perform single crystal XRD studies and powder X-ray diffraction (PXRD) study was carried out using a powder X-ray diffractometer (PANalytical Model, Nickel filtered Cu K_α radiations with $\lambda = 1.54056 \text{ \AA}$ at 35 kV, 10 mA) in the diffraction angle range $10^\circ - 80^\circ$. To carry out the second-order nonlinear optical property, Kurtz and Perry powder SHG test was carried out for the powdered sample of LAAP using Nd:YAG Q-switched laser which emits the first harmonic output of 1064 nm. The optical transmission spectrum of LAAP crystal has been recorded in the region 190-1100 nm using a Perkin Elmer (Model: Lambda 35) UV-vis-NIR spectrophotometer. For this study, an optically polished single crystal of thickness 1.5 mm was used. The measurements of dielectric constant and dielectric loss for the grown LAAP single crystal were carried out using an LCR meter (Agilent 4284A) at various frequencies in the range $10^2 - 10^6 \text{ Hz}$ and at different temperatures ranging from 30° to 90°C . For the good ohmic contact, opposite faces of the sample crystal were coated with good quality graphite paint. For etching studies, the sample crystal of LAAP was immersed in the selected etchant for known duration of time and dried with the aid of a tissue paper. The revealed etch features were analyzed using an optical microscope attached with a camera (Olympus make). The third-order NLO property of LAAP crystal was investigated using Z-scan technique and in this measurement, a He-Ne laser ($\lambda = 632.8 \text{ nm}$) was

used as the light source and focused by a lens of 22.5 cm focal length. LAAP crystal of thickness 1 mm was translated across the focal region along the axial direction, which was the direction of the propagation of the laser beam. The transmission of the beam through an aperture placed in the far field was measured using photodetector fed to the digital power meter.

4. Results and discussion

4.1 X-ray diffraction (XRD) studies

The structural characterization was carried out by single crystal XRD and powder XRD studies. The grown LAAP crystal has been subjected to single crystal X-ray diffraction study to obtain the crystallographic data which reveals that LAAP crystal crystallizes in monoclinic structure. The obtained lattice parameters for the LAAP crystal are $a = 8.263(3) \text{ \AA}$, $b = 7.515(2) \text{ \AA}$, $c = 15.536(4) \text{ \AA}$, $\alpha = 90^\circ$, $\beta = 106.15^\circ$, $\gamma = 90^\circ$ $V = 926.65 (\text{ \AA})^3$. The obtained single crystal XRD data are found to be in good agreement with the data reported in the literature [13]. The grown LAAP crystal has been crushed to a uniform fine powder and subjected to powder X-ray diffraction to identify the diffraction planes and hence the lattice parameters. The powder XRD pattern of LAAP sample is presented in the Fig. 2. All the reflection peaks of powder XRD pattern of grown crystal were indexed using the INDEXING and TREOR software packages following the procedure of Lipson and Steeple [14]. The powder XRD data for LAAP sample are provided in the Table 1.

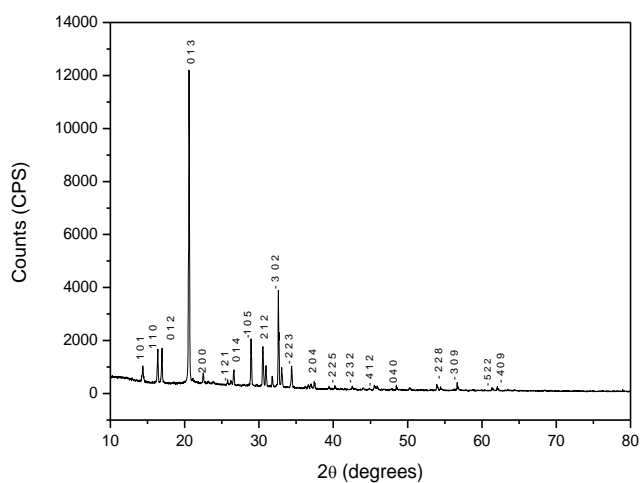


Fig. 2. Powder XRD pattern for LAAP sample.

Table 1. Powder XRD data for LAAP sample.

2 θ (deg.)		d (\AA)		Rel. int. (%)	h k l
Observed	Calculated	Observed	Calculated		
14.365	14.042	6.161	6.302	4.940	1 0 1
16.387	16.242	5.405	5.453	10.42	1 1 0
16.951	16.731	5.226	5.294	11.27	0 1 2
20.590	21.408	4.310	4.147	100.00	0 1 3
22.480	22.429	3.952	3.961	3.51	2 0 0
25.782	26.183	3.453	3.401	1.74	-1 2 1
26.628	26.662	3.345	3.341	4.99	0 1 4
28.927	28.842	3.084	3.093	15.14	-1 0 5
30.528	30.743	2.926	2.906	12.57	2 1 2
31.763	31.548	2.815	2.834	3.39	1 1 4
32.608	32.617	2.744	2.743	31.19	-3 0 2
33.039	32.823	2.709	2.726	6.01	2 2 0
34.388	34.291	2.606	2.613	6.91	-2 2 3
37.466	37.447	2.398	2.400	1.38	2 0 4
40.211	40.234	2.241	2.240	1.15	-2 2 5
42.551	42.560	2.123	2.122	0.98	-2 3 2
45.514	45.558	1.991	1.989	1.48	-4 1 2
48.480	48.395	1.876	1.879	1.16	0 4 0
53.932	53.896	1.699	1.700	1.90	-2 2 8
54.441	54.387	1.684	1.686	1.19	-1 4 4
56.671	56.629	1.623	1.624	2.47	-3 0 9
61.352	61.428	1.510	1.508	1.01	-5 2 2
62.070	62.068	1.494	1.494	1.30	-4 0 9

4.2 EDAX studies

EDAX stands for Energy Dispersive Analysis by X-rays and it is a technique used for identifying the elemental composition of the specimen. It works as an integrated feature of a scanning electron microscope (SEM). During EDAX analysis, the specimen is bombarded with an electron beam inside the scanning electron microscope and X-rays will be emitted. By measuring the amounts of energy present in the X-rays being released by the sample during electron beam bombardment, the identity of the atom from which the X-ray was emitted can be established. In this work, the EDAX spectrum of the LAAP sample was recorded using a computer controlled scanning electron microscope (Model: HITACHI S-3000 H) and it is displayed in Fig. 3. From the diagram, it is confirmed that the elements such as C, O and N are present in the sample.

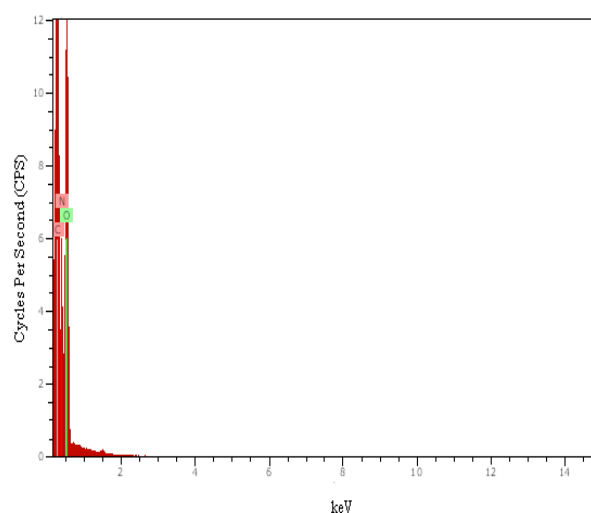


Fig. 3. EDAX spectrum of LAAP crystal.

4.3 Optical transmission spectral analysis

The optical transmission range, transparency cut-off and the absorbance band are the most important optical parameters for laser frequency conversion applications. The UV-visible transmittance spectrum of LAAP crystal is

shown in the Fig. 4. From the spectrum, it is noticed that the LAAP crystal is quite transparent from 1100 nm to 450 nm and therefore the crystal of this work is transparent for green light and thus it is a second harmonic generator for Nd:YAG laser. The energy gap value is determined for the lowest cut-off wavelength value of ($\lambda = 445$ nm), which is equal to 2.78 eV.

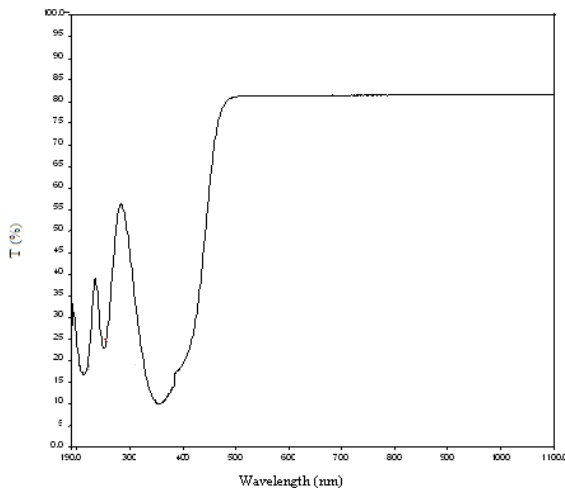


Fig. 4. UV-visible transmittance spectrum of LAAP crystal.

4.4 Second-order and third-order NLO studies

The famous Kurtz and Perry powder technique [15] was used to check the second-order nonlinear optical (NLO) activity of LAAP sample. A high intensity Nd:YAG laser ($\lambda = 1064$ nm) with a pulse duration of 6 ns was passed through the powdered sample of LAAP (particle size of 150 μm) and the emission of green radiation of wavelength 532 nm confirms SHG. The second harmonic generation signal of 12.97 mJ for LAAP crystal was obtained for an input energy of 0.68 J. But the standard KDP sample gave an SHG signal of 8.8 mJ for the same input energy. Thus, it is observed that the SHG efficiency of the LAAP sample is 1.47 times that of the standard KDP crystal.

Third-order NLO studies were carried out by using Z-scan technique. It is a standard technique for determining the nonlinear index of refraction (n_2), nonlinear susceptibility and nonlinear absorption coefficient (β) of samples [16]. Measurements of open and closed aperture of the normalized transmittance and sample position Z have been made and the curves are shown in Figs. 5 and 6. The curves are characterized by a prefocal transmittance maximum (peak) followed by a postfocal transmittance minimum (valley) intensity. The transmission difference between peak and valley (ΔT_{p-v}) is written in terms of phase shift

$$\Delta T_{p-v} = 0.406 (1-s)^{0.25} |\Delta\phi|$$

Linear transmittance aperture (S) is calculated using the relation

$$S = 1 - \exp\left(\frac{-2r_a^2}{\omega_a^2}\right)$$

where r_a is the radius of the aperture and ω_a is the beam radius at the aperture. The third-order nonlinear refractive index (n_2) of the crystal was calculated by following the relation.

$$n_2 = \Delta\phi / (K I_0 L_{\text{eff}})$$

where I_0 is the intensity of the laser beam at the focus ($Z = 0$) and $K = 2\pi/\lambda$ (λ is the wavelength of laser beam).

The effective thickness can be calculated using the relation

$$L_{\text{eff}} = [1 - \exp(-\alpha L)] / \alpha$$

where α is the linear absorption coefficient and L is the thickness of the sample. The nonlinear absorption coefficient (β) can be calculated using the following relation

$$\beta = \frac{2\sqrt{2}\Delta T}{I_0 L_{\text{eff}}}$$

where ΔT is the one peak value at the open aperture Z-scan curve. The real and imaginary parts of the third order nonlinear optical susceptibility ($\chi^{(3)}$) are defined as

$$\text{Real part of } \chi^{(3)} = (10^{-4} \epsilon_0 c^2 n_0^2 n_2) / \pi \quad (\text{esu})$$

$$\text{Imaginary part of } \chi^{(3)} = (10^{-2} \epsilon_0 c^2 n_0^2 \lambda \beta) / 4\pi^2 \quad (\text{esu})$$

$$\text{Absolute value of } \chi^{(3)} = [\{\text{Real part of } \chi^{(3)}\}^2 + \{\text{Imaginary part of } \chi^{(3)}\}^2]^{1/2} \quad (\text{esu})$$

Here ϵ_0 is the vacuum permittivity, n_0 is the linear refractive index of the sample and c is the velocity of the light in vacuum. The obtained results from the Z-scan measurements for LAAP crystal are presented in Table 2. The positive value of third-order nonlinear refractive index (n_2) is $0.65 \times 10^{-10} \text{ cm}^2/\text{W}$ and it indicates that the sample is in self-focusing nature. The value of nonlinear absorption coefficient (β) for LAAP crystal is $0.19 \times 10^{-4} \text{ cm/W}$ and it indicates the two-photon absorption process in the sample. The absolute value of nonlinear susceptibility for LAAP crystal is $0.803 \times 10^{-6} \text{ esu}$ and this reflects the third-order NLO activity of the sample.

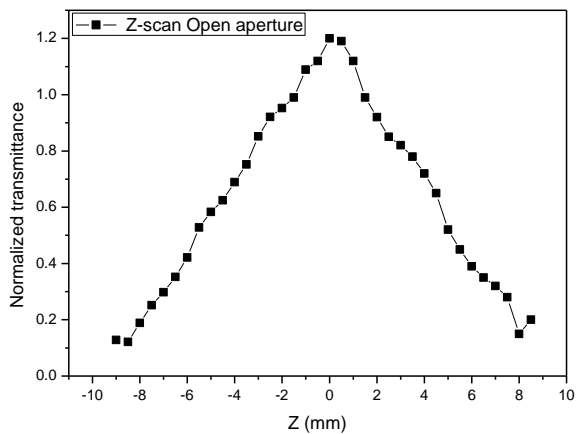


Fig. 5.

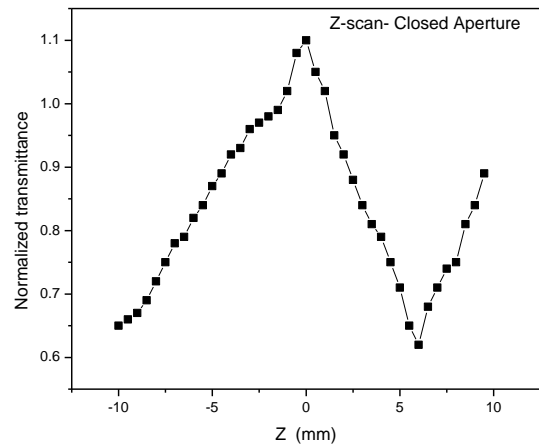


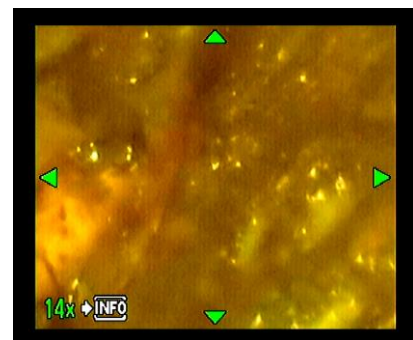
Fig. 6.

Table 2. Obtained data from Z-scan measurements for LAAP crystal.

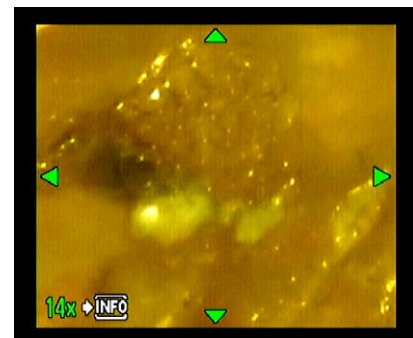
Nonlinear refractive index (n_2)	$0.65 \times 10^{-10} \text{ cm}^2/\text{W}$
Nonlinear absorption coefficient (β)	$0.19 \times 10^{-4} \text{ cm/W}$
Real part of the third-order nonlinear susceptibility $\text{Re}(\chi^{(3)})$	$0.55 \times 10^{-8} \text{ esu}$
Imaginary part of the third-order nonlinear susceptibility $\text{Im}(\chi^{(3)})$	$8.04 \times 10^{-7} \text{ esu}$
The third-order nonlinear susceptibility ($\chi^{(3)}$)	$0.803 \times 10^{-6} \text{ esu}$

4.5 Etching studies

Etching property is used as the most convenient method for visualization of defects. In the present work, water was used as an etchant. In the process of chemical etching, the etching time, concentration of etchant and selective etchant are playing vital roles. The etching studies were carried out on the (001) plane of the single crystal of LAAP with de-ionized water as an etchant using an optical microscope attached with a camera at room temperature for etching times of 10 s and 20 s. The etching features of LAAP crystal are presented in the Fig. 7. Etching of the grown LAAP crystal for 10 s produces small dot-shaped etch pits. On successive etching for 20 s produces more number of circle-shaped pits and some valley-shaped edge pits in the sample. Since LAAP crystal is soluble in water, more number of pits are seen when etchant time is increased. The resulting etch pits are the characteristic distribution of defects and are produced at the dislocation sites [31].



(a)



(b)

Fig. 7. Etch pit patterns of LAAP sample.

4.6 Dielectric constant, loss factor and activation energy

Figs. 8 and 9 present the variations of dielectric constant and dielectric loss factor with temperature at frequencies such as 10^2 , 10^3 and 10^6 Hz. From the results, it is observed that both the dielectric parameters (ϵ_r and $\tan \delta$) increase as the temperature increases and these values decrease as frequency decreases for LAAP crystal. The high values of ϵ_r at low frequencies may be attributed to dominance of space charge polarization and the nature of decrease of dielectric constant and dielectric loss with frequency suggests that the LAAP crystal seem to contain dipoles of continuously varying relaxation times. It is observed that LAAP crystal has low dielectric constant and low dielectric loss at higher frequencies and hence suitable for electro-optic applications. AC conductivity (σ_{ac}) of LAAP crystal for different frequencies can be determined using the relation $\sigma_{ac} = \omega \epsilon_r \epsilon_0 \tan \delta$ where ω is the angular frequency of a.c. supply, ϵ_r is the dielectric constant, ϵ_0 is the permittivity of free space, $\tan \delta$ is the dielectric loss factor. The AC conductivity values are fitted in the equation $\sigma_{ac} = \sigma_0 \exp(-E / kT)$ where σ_0 is a constant which depends upon the type of the sample, E is the activation energy, k is the Boltzmann's constant and T is the absolute temperature [17]. A graph is drawn between $\ln \sigma_{ac}$ and $1000/T$ at frequencies such as 10^2 , 10^3 and 10^6 Hz (Fig. 10) and the activation energy was calculated by linear fit analysis. It is to be mentioned here that the graphs of $\ln \sigma_{ac}$ and $1000/T$ were drawn using the ORIGIN software package at frequencies 10^2 , 10^3 and 10^6 Hz separately. Then, the three graphs were combined into one graph and it is shown in Fig. 10. Activation energy values were determined from each graph separately and are provided in the Table 3. From the results, it is noticed that the values of AC conductivity increases with temperature and also with frequency. The values of activation energy are found to be slightly decreasing with frequency (almost independent of frequency) and the decrease in activation energy for LAAP crystal may be attributed with high conductivity of the sample at higher frequencies.

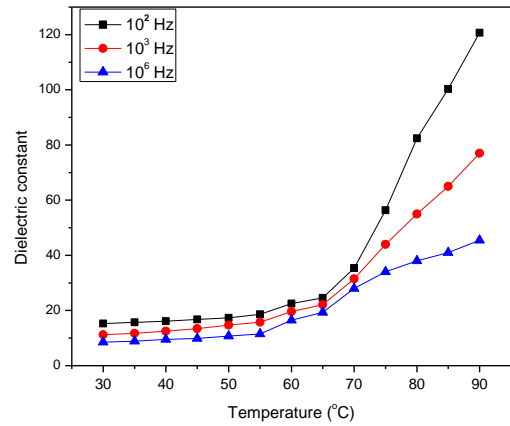


Fig. 8. Temperature dependence of dielectric constant for LAAP crystal.

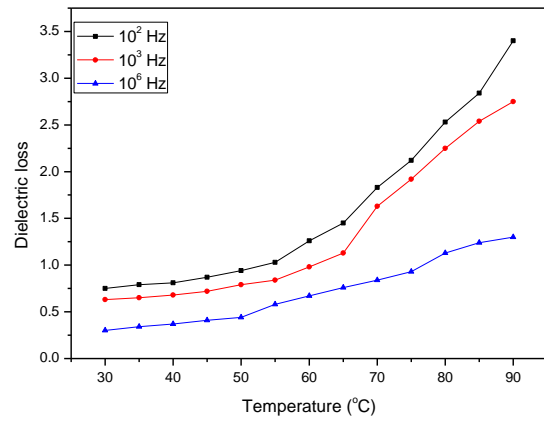


Fig. 9. Temperature dependence of dielectric loss for LAAP crystal.

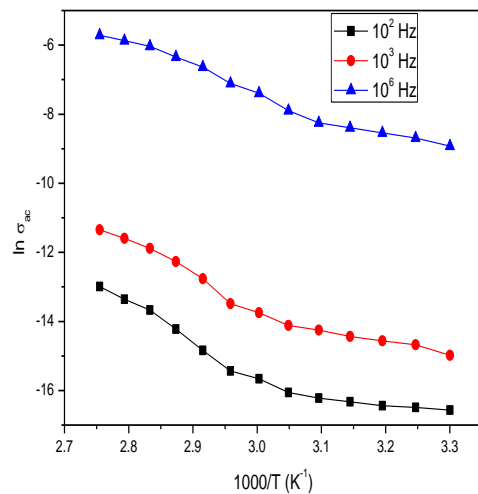


Fig. 10. Plots of $\ln \sigma_{ac}$ versus $1/T$ at different frequencies for LAAP crystal.

Table 3. Some pertinent data of AC conductivity and activation energy for LAAP crystal.

Frequency (Hz)	AC conductivity			Activation Energy (eV)
	$\sigma_{ac} \times 10^{-6}$ (ohm m) ⁻¹ 40 °C	60 °C	80 °C	
10 ²	0.0725	0.157	1.159	0.595
10 ³	0.4726	1.068	6.881	0.589
10 ⁶	195.4450	614.692	2387.598	0.581

5. Conclusion

L-alanine alaninium picrate (LAAP) salt was synthesized by solution method and the single crystals were grown by slow evaporation technique and the harvested crystals are observed to be yellow in colour, transparent and non-hygroscopic. EDAX study reveals the presence of C, N, O elements in grown LAAP crystal. XRD studies confirms the monoclinic structure of the grown crystal. The optical transmittance study reveals high transparency of the crystal in the range 450-1100 nm with a cut off wavelength of 445 nm. SHG efficiency of LAAP sample was found to be 1.47 times that of KDP crystal. Etching studies reveal that dot and valley shaped etch pits in the grown crystal. Dielectric studies were used to obtain values of dielectric constant, dielectric loss, AC conductivity and hence activation energy for LAAP crystal in order to understand the conduction processes that are taking place in the sample. Z-scan technique was used to analyze the third-order parameters which reveal that LAAP crystal possess self-focusing nature and two-photon absorption process.

Acknowledgement

The authors are grateful to Department of Science and Technology (DST), Government of India for the financial support to carry out this work. The authors like to thank the supported work from various research centers such as M.K. University (Madurai), M.S. University (Tirunelveli), St Joseph College (Trichy), Crescent Engineering College (Chennai) and S. T. Hindu College (Nagercoil). Also the authors are thankful to the management of Aditanar College of Arts and Science, Tiruchendur for the encouragement given to us to carry out the research work.

References

- [1] L. Misoguti, A. T. Varela, F. D. Nunes, V. S. Bagnato, F. F. A. Melo, J. Mendes Filho, S. C. Zilio, *Opt. Mater.* **6**, 147 (1996).
- [2] P. Selvarajan, J. Glorium Arul Raj, S. Perumal, J. *Crystal Growth* **311**(15), 3835 (2009).
- [3] K. K. Hema Durga, P. Selvarajan, D. Shanthi, *Int. J. Curr. Res. Rev.* **4**(14), 68 (2012).
- [4] K. J. Arun, S. Jayalekshmi, *J. Mineral. Mater. Charact. Engin.* **8**(8), 635 (2009).
- [5] C. Razzetti, M. Ardoino, L. Zanotti, M. Zha, C. Parorici, *Cryst. Res. Technol.* **37**, 456 (2002).
- [6] D. Rajan Babu, D. Jayaraman, R. Mohan Kumar, R. Jayavel, *J. Crystal Growth* **245**, 121 (2002).
- [7] C. Justin Raj, S. Jerome Das, *J. Crystal Growth* **304**, 191 (2007).
- [8] A. S. J. Lucia Rose, P. Selvarajan, S. Perumal, *Mater. Chem. Phys.* **130**, 950 (2011).
- [9] C. Ramachandra Raja, G. Gokila, A. Antony Joseph, *Spectrochimica Acta Part A* **72**(4), 753 (2009).
- [10] D. Prabha, S. Palaniswamy, *Int. J. Chem. Environ. Pharma. Res.* **1**(1), 54 (2010).
- [11] A. Aravindan, P. Srinivasan, N. Vijayan, R. Goplakrishnan, P. Ramasamy, *Spectrochimica Acta Part A* **71**(2), 297 (2008).
- [12] N. Vijayan, G. Bhagavannarayana, K. K. Maurya, S. N. Sharma, R. Gopalakrishnan, J. Jayabharathid, P. Ramasamy, *Optik* **123**(7), 604 (2012).
- [13] V. V. Ghazaryan, M. Fleck, A. M. Petrosyan, *J. Molecular Structure* **1015**, 51 (2012).
- [14] H. Lipson, H. Steeple, Fifth ed. Macmillan, New York, 1970.
- [15] S. K. Kurtz, T. Perry, *J. Appl. Phys.* **39**(8), 3798 (1968).
- [16] T. C. Sabari Girisun, S. Dhanuskodi, *Cryst. Res. Technol.* **44**, 1297 (2009).
- [17] P. Selvarajan, J. Glorium Arulraj, S. Perumal, *Physica B* **405**, 738 (2010).

*Corresponding author: pselvarajanphy@yahoo.co.in